DOI: 10.1161/CIRCULATIONAHA.115.009800

Pathogenesis of the Novel Autoimmune-Associated Long QT Syndrome

Running title: *Yue et al.; Anti-Ro antibodies and Long QT syndrome*

Yuankun Yue, MD[1]; Monica Castrichini, PhD[2]; Ujala Srivastava, PhD [1,3]; Frank Fabris, BS[1,3]; Krupa Shah, MS[1]; Zhiqiang Li, PhD[1,3]; Yongxia Qu, MD/PhD[1,3]; Nabil El-Sherif, MD[1]; Zhengfeng Zhou, MD/PhD[4]; Craig January, MD/PhD[5]; M. Mahmood Hussain, PhD[1,3]; Xian-Cheng Jiang, MD[1,3]; Eric A Sobie, PhD[6]; Marie Wahren-Herlenius, MD[7]; Mohamed Chahine, PhD[8]; Pier-Leopoldo Capecchi, MD[2]; Franco Laghi-Pasini, MD[2]; Pietro-Enea Lazzerini, MD[2]; Mohamed Boutjdir, PhD[1,3,9]

[1]Cardiovascular Research Program, VA New York Harbor Healthcare System, Brooklyn, NY; [2]Dept of Medical Sciences, Surgery and Neurosciences, University of Siena, Siena, Italy; [3]Depts of Medicine, Cell Biology and Pharmacology, State University of New York Downstate Medical Center, Brooklyn, NY; [4]Knight Cardiovascular Institute, Oregon Health & Science University, Portland, OR; [5]Division of Cardiovascular Medicine, Dept of Medicine, University of Wisconsin, Madison, WI, [6]Pharmacology and Systems Therapeutics, Icahn School of Medicine at Mount Sinai, New York, NY, [7]Unit of Experimental Rheumatology, Department of Medicine, Karolinska Institute, Stockholm, Sweden; [8]Centre de Recherche de l'Institut Universitaire en Santé Mentale de Québec, Laval University, Quebec City, QC, Canada; [9]Dept of Medicine, New York University School of Medicine, New York, NY

Address for Correspondence:

Mohamed Boutjdir, PhD

VA New York Harbor Healthcare System

Research and Development Office (151)

800 Poly Place

Brooklyn, NY 11209

Tel: 718 630 2891

Fax: 718 630 3796

E-mail: mohamed.boutjdir@va.gov

Journal Subject Code: Basic science research:[132] Arrhythmias - basic studies

DOI: 10.1161/CIRCULATIONAHA.115.009800

Abstract

Background—Emerging clinical evidence demonstrates high prevalence of QTc prolongation and complex ventricular arrhythmias in patients with anti-Ro antibody (anti-Ro Ab) positive autoimmune diseases. We tested the hypothesis that anti-Ro Abs target the HERG K^+ channel which conducts the rapidly activating delayed K^+ current, I_{Kr}, thereby causing delayed repolarization seen as QT interval prolongation on the electrocardiogram (ECG).

Methods and Results—Anti-Ro Ab positive sera, purified IgG and affinity purified anti-52kDa Ro Abs from patients with autoimmune diseases and QTc prolongation were tested on I_{Kr} using HEK293 cells expressing HERG channel and native cardiac myocytes. Electrophysiological and biochemical data demonstrate that anti-Ro Abs inhibit I_{Kr} to prolong action potential duration by directly binding to the HERG channel protein. 52kDa Ro antigen immunized guinea-pigs showed QTc prolongation on ECG after developing high titers of anti-Ro Abs which inhibited native I_{Kr} and cross-reacted with guinea-pig ERG channel.

Conclusions—The data establish that anti-Ro Abs from patients with autoimmune diseases inhibit I_{Kr} by cross-reacting with the HERG channel likely at the pore region where homology between 52Ro antigen and HERG channel is present. The animal model of autoimmune-associated QTc prolongation is the first to provide strong evidence for a pathogenic role of anti-Ro Abs in the development of QTc prolongation. Together, it is proposed that adult patients with anti-Ro Abs may benefit from routine ECG screening and those with QTc prolongation should receive counselling about drugs that may increase the risk for life threatening arrhythmias.

Key words: antibody, long QT syndrome, arrhythmia, immune system, ion channels

DOI: 10.1161/CIRCULATIONAHA.115.009800

Introduction

The Long QT syndrome (LQTS) is one of the most studied channelopathies where abnormal prolongation of ventricular repolarization predisposes to the life threatening ventricular arrhythmia Torsade de Pointes[1-4]. LQTS can be congenital or acquired. While congenital LQTS is caused by mutations in ion channel protein coding genes, acquired LQTS is often drug-induced[3, 5, 6]. In most cases of drug-induced QT prolongation, the target ion channel is the Human ether-a-go-go-related gene (HERG) encoding the pore-forming subunits (Kv11.1) of the rapidly activating delayed K^+ channel conducting I_{Kr}[1, 3-5]. I_{Kr} plays a major role during repolarization of the cardiac action potential (AP)[4,6]. Its reduction by drug block or genetic defects causes delayed repolarization of the AP which manifests as prolongation of the QT interval on the ECG[1, 3, 4, 6].

A novel acquired autoimmune-associated LQTS has been recently reported in adult patients carrying anti-Ro antibodies (anti-Ro Abs)[7-10] which result from an autoimmune response against the intracellular ribonucleoprotein, SSA/Ro antigen (Ro). The detection of circulating anti-Ro Abs is relatively frequent in the course of autoimmune diseases, particularly Sjogren's syndrome, and systemic lupus erythematosus, but also in other connective tissue diseases (CTD) including mixed CTD, undifferentiated CTD, polymyositis/dermatomyositis, systemic sclerosis, rheumatoid arthritis and even primary biliary cirrhosis [11, 12]. Interestingly, in the adult patients, anti-Ro Ab positivity is associated with repolarization abnormalities (QTc prolongation) [7-10], but not with conduction abnormalities (complete atrio-ventricular block) which is well described in children born to mothers with anti-Ro Abs[13, 14]. Accordingly, it is assumed that the adult heart does not represent an immunological target for anti-Ro Abs. However, emerging clinical observations suggest that anti-Ro Abs may be arrhythmogenic for the adult heart by causing QT

interval prolongation[7-10]. Specifically, in a cohort of CTD patients, *more than half (58%)* of patients with anti-Ro Abs displayed a prolonged QTc, with a mean QTc duration significantly longer in anti-Ro Ab positive vs. anti-Ro Ab negative patients [7]. In a subsequent study, patients with CTD and anti-Ro Ab showed *five-fold* higher incidence of complex ventricular arrhythmias compared with anti-Ro Ab negative patients[9]. Despite this high incidence of QTc prolongation and ventricular arrhythmias in patients with CTD, the pathogenesis of this autoimmune associated QTc prolongation in the adult remains poorly understood.

Methods

Study Population

Six CTD patients' sera were studied (see **Table 1**). Three CTD patients were anti-Ro Abs positive with QTc>460 ms and three CTD patients were anti-Ro Abs negative with QTc<460 ms[15]. Patients did not have echocardiographic abnormalities and/or evidence of organic heart diseases, diabetes mellitus, renal failure, thyroid disease or electrolyte abnormalities[7, 9] and none were taking drugs that can potentially affect the QT interval. Genetic testing for mutations in the KCNH2, KCNQ1, SCN5A, KCNE2, KCNE1 and KCNJ2 genes was negative in the three anti-Ro Abs positive patients studied. The Institutional Review Board approved the consent process for study participants and patients gave informed consent. ECG recordings are described in supplemental methods.

Purification of IgG and affinity purification of anti-52kDa/Ro antibodies from patients' sera

IgG and affinity purification of anti-52kDa/Ro (52Ro) Abs were performed as previously described with modifications[16, 17] and detailed in supplemental Methods.

DOI: 10.1161/CIRCULATIONAHA.115.009800

Electrophysiology using HEK293 cells stably expressing HERG channel and guinea-pig ventricular myocytes

Details of DNA constructs and the methods of stable transfection of HEK293 cells with HERG channel were reported elsewhere[18] and the electrophysiology recording and single ventricular myocytes enzymatic dissociation technique are detailed in the supplemental Methods and as previously described[19].

Western blots analysis

Western blot experiments were performed as described in supplemental Methods.

Guinea-pigs immunization

Seven adult guinea-pigs (5 females and 2 males) were immunized with recombinant 52kD Ro antigen (Sigma), initially at day1 followed by boosters at days 14, 28 and 42 as described in supplemental methods and as previously reported with modification [16, 20-22].

ELISA

Sera from each immunized guinea-pig were analyzed for anti-Ro Ab reactivity by ELISA as previously described[16, 20] with some modifications reported in supplemental methods.

Statistical Analysis

Statistical comparisons were evaluated with paired Student's t-test and with nonparametric Wilcoxon paired test as appropriate. Data are presented as mean±SEM. A value of $p<0.05$ was considered significant.

Results

Anti-Ro Ab positive sera from patients with QTc prolongation inhibit I_{Kr}

We first tested the electrophysiological effect of whole serum containing anti-Ro Abs from a

patient who has CTD and a long QTc of 566 ms (**Figure 1A**). **Panel B** shows the voltage protocol used to record I_{Kr}. Anti-Ro Ab positive serum #1 (200 µl; 83 U/ml) inhibited both the peak and tail of I_{Kr} recorded from HEK293 cells stably expressing the HERG channel (**Figure 1C-F**). Selected current traces are shown before (panel C) and after the application of anti-Ro Ab positive serum (**panel D**). The I-V relationships for I_{Kr} peak and tail before and after the application of anti-Ro Ab positive serum are shown in panels E (n=10) and F (n=10), respectively. Anti-Ro Ab positive serum significantly reduced I_{Kr} peak density by 40.4% from 53.9± 5.1 pA/pF to 32.1± 5.2 pA/pF at -10 mV ($p<0.0001$, n=10) and reduced I_{Kr} tail density by 38.4% from 93.4±8.7 pA/pF to 57.5±10.2 pA/pF at -10 mV ($p<0.0001$, n=10). To ensure reproducibility of I_{Kr} inhibition, sera from two additional anti-Ro Abs positive CTD patients with QTc of 514 ms and 498 ms respectively were tested (**Table 1**). The results show that serum #2 (200 µl, 241U/ml) and serum #3 (200 µl, 241U/ml) both significantly ($p<0.0001$, n=10 each) inhibited I_{Kr} peak and tail densities (**panel G**).

Anti-Ro Ab negative sera from patients with normal QTc did not affect I_{Kr}

Next, we demonstrated that anti-Ro Ab negative serum #4 (200 µl) from a control patient with a normal QTc of 404 ms (**Figure 2A**) had no effect on I_{Kr}. **Figure 2** shows selected I_{Kr} traces before (B) and after (C) the application of anti-Ro Ab negative serum. Panels D and E show I-V relationships of I_{Kr} peak and tail densities before and after the application of anti-Ro Ab negative serum (n=10) respectively. I_{Kr} peak densities before and after the application of anti-Ro Ab negative serum at -10 mV were 56.9± 6.4 pA/pF vs. 53.1±6.8 pA/pF ($p=0.08$), n=10) and I_{Kr} tail densities were 94.5±9.2 pA/pF vs. 89.2±7.3 pA/pF ($p=0.09$, n=10). Similarly, additional sera from two anti-Ro negative CTD patients with QTc of 451 ms and 430 ms respectively (**Table 1**) had no significant effect on I_{Kr} peak or tail current densities (**Panel F**).

DOI: 10.1161/CIRCULATIONAHA.115.009800

Anti-Ro Ab positive purified IgG from patients with long QTc inhibits I_{Kr}

The effect of purified IgG containing anti-Ro Abs from serum #1 was tested on I_{Kr}. **Figure 3** shows that purified IgG (75 μg/ml) significantly inhibited both I_{Kr} peak and tail densities at several tested voltages. I_{Kr} peak density at -10 mV decreased by 33.1% from 50.1±4.0 pA/pF to 33.6±3.8 pA/pF ($p<0.0001$, n=10) and I_{Kr} tail density decreased by 35.4% from 95.5±5.4 pA/pF to 61.7±5.7 pA/pF ($p<0.0001$, n=10) upon IgG application. The dose-dependent effect of IgG on I_{Kr} is shown in **Figure 4A**. Anti-Ro Abs positive IgG inhibited I_{Kr} peak density in dose-dependent manner (n=6) with an EC_{50}=87.3 μg/ml. **Figure 4B** shows a representative time course for I_{Kr} peak inhibition by anti-Ro Abs positive IgG (75 μg/ml). IgG inhibited I_{Kr} peak in a time-dependent manner with a steady state effect reached after 8 min after IgG application. The inhibition of I_{Kr} by IgG was only partially reversible (washout). **Figure 4C** shows that anti-Ro Ab negative IgG at -10 mV did not significantly inhibit I_{Kr} peak densities (from 49.4±7.1 pA/pF to 46.3±5.2 pA/pF, n=6, p=0.1) or I_{Kr} tail densities (from 92.2±7.4 pA/pF to 88.3±8.1 pA/pF, n=6, p=0.09). **Figure 4D** illustrates the time course of I_{Kr} peak without any intervention and shows minimal rundown seen in six experiments. To investigate whether the above IgG containing anti-Ro Abs inhibition of I_{Kr} occurs by affecting HERG channel's kinetics, the activation and deactivation time constants (τ) were fitted by Boltzmann' equation. **Figure 4E and 4F** demonstrate that both activation and deactivation were best fit by a single exponential and that anti-Ro Ab positive IgG did not affect HERG channel's kinetics at all voltages (n=10, p=0.1).

Anti-Ro Ab positive IgG but not anti-Ro Ab negative IgG, cross-react with HERG channels

To test whether the inhibition of I_{Kr} by anti-Ro Abs positive IgG is due to a direct interaction with the HERG channel protein, Western blot experiments were performed using proteins from

HEK293 cells stably expressing HERG channels (n=6) and un-transfected HEK293 cells (negative control, n=6). **Figure 5A** shows that anti-Ro Ab positive IgG did not recognize any bands in un-transfected HEK293 cells (lane 1) but recognized two bands at about 155 kDa and 135 kDa (lane 2) corresponding to the glycosylated and endoplasmic reticulum-retained HERG channel consistent with previous reports [18, 23]. **Figure 5B** shows no bands when anti-Ro Abs negative IgG was used in both un-transfected HERG cells (lane 3) and transfected HEK293 cells expressing HERG channels (lane 4). Similar to anti-Ro Ab positive IgG in **Figure 5A** (lane 1), the use of a commercial anti-Kv11.1 Ab did not recognize any bands from un-transfected tsA201 cells (**Figure 5C**, lane 5, negative control) but did recognize the bands corresponding to the HERG channel (lane 6).

Affinity purified anti-52kDa Ro Abs from patient with long QTc inhibits I_{Kr}

To demonstrate the specificity anti-Ro Abs' effect on I_{Kr}, affinity purified anti-52Ro Abs from sera #1 were tested on I_{Kr}. Similar to purified IgG, affinity purified anti-52Ro Abs (52µg/ml) significantly inhibited I_{Kr} peak densities by 28.5% (from 35.4±2.6 pA/pF to 25.3±2.4 pA/pF, n=10, p<0.0001) and I_{Kr} tail densities by 30.5% (from 62.7±5.9 to 43.5±4.7, n=10, p<0.0001). **Figure 6** shows current tracings (panels A and B), I-V relationships (**panels C and D**) and dot plot (**panels E**) before and after the application of affinity purified anti-52Ro Abs.

Immunization of adult guinea-pigs with SSA/52kDa Ro antigen causes QTc prolongation

To further demonstrate the potential role of anti-Ro Abs in the pathogenesis of QTc prolongation, we sought to establish an animal model of anti-Ro Abs induced QTc prolongation. The guinea-pig is a suitable animal model for QT studies because of the similarities of ECG features with Humans[24, 25]. The results in **Table 2** show significant QTc prolongation and high titers of anti-Ro Abs after immunization in seven guinea-pigs. No significant differences in heart

DOI: 10.1161/CIRCULATIONAHA.115.009800

rate, PR intervals and QRS durations were observed before and after immunization. **Figure 7** illustrates ECGs from a guinea-pig before (panel A) and after immunization with a ΔQTc of 36 ms (panel B). If the QTc prolongation seen in the immunized guinea-pigs is due, at least in part, to anti-Ro Ab's inhibition of I_{Kr}, then anti-Ro Abs should be expected to also lengthen the ventricular AP duration (APD). Thus, APs were recorded from guinea-pig single ventricular myocytes before and after the application of anti-Ro positive IgG at 0.5 Hz in the current clamp mode configuration. **Figure 7C** shows APs before (left panel) and after the application of anti-Ro Ab positive IgG (75 μg/ml, right panel). Anti-Ro Ab positive IgG resulted in a prolongation of the APD at 90% (APD_{90}) by 39.7% without any changes in the resting membrane potential or the AP amplitude. Averaged data from a total of 6 experiments are shown in the lower panel of **Figure 7C**. Anti-Ro Ab negative IgG did not have any significant effects on APD_{90} (348.4±32.1 ms before and 350.2±39.3 ms after negative IgG, p=0.1, n=6). **Figure 7D** shows I_{Kr} recorded from guinea-pig ventricular myocytes using a short (200 ms) duration pulse protocol from a holding potential of -40 mV where the slow delayed rectifier, I_{Ks} is still inactive (and in the presence of 10 μM chromanol). Consistent with the observed APD lengthening, anti-Ro Ab positive IgG (75 μg/ml), but not control anti-Ro Ab negative IgG (75 μg/ml), inhibited I_{Kr} peak by 30.8% and I_{Kr} tail by 28.9% (dot plot in lower panel D, n=6, p<0.0001). To test whether the observed functional inhibition of I_{Kr} is through direct interaction with the guinea-pig Kv11.1 (gpERG) channel proteins, Western blots experiments were performed. Anti-Ro Ab positive IgG cross-reacted with the endogenous Kv11.1 proteins from guinea-pig ventricles (**Figure 7E**, lane 3) and HEK293 cells expressing HERG/Kv11.1 channel (lane 2) but did not show reactivity to un-transfected HEK293 cells (lane 1, negative control). The commercial anti-Kv11.1 Ab also recognized the same protein bands in guinea-pig ventricles (lane 6) and HEK293 cells expressing

HERG channel (lane 5) but not un-transfected HEK293 cells as did anti-Ro Ab positive IgG (lane 3).

Figure 8A shows that anti-Ro Ab positive serum from immunized guinea-pigs inhibited I_{Kr} expressed in HEK293 cells. Anti-Ro Abs positive serum (100 µl) from immunized guinea-pigs inhibited I_{Kr} peak densities by 29% (from 44.6±6.1 pA/pF to 32.5±5.2 pA/pF, p<0.0001, n=6) and I_{Kr} tail densities by 28% (from 20.1±3.1 pA/pF to 14.3±2.4 pA/pF, p<0.0001, n=6). These effects on I_{Kr} were not seen with anti-Ro Abs negative serum from pre-immunized guinea-pigs (I_{Kr} peak densities from 38.2±5.1 pA/pF to 35.4±4.1 pA/pF, p=0.1, n=6; I_{Kr} tail from 19.4±3.1 pA/pF to 17.5±3.3 pA/pF, p=0.1, n=6). Using guinea-pig ventricles, anti-Ro Abs positive (lane 1) but not anti-Ro Ab negative serum (lane 2) above recognized Kv11.1 proteins.

Homology analysis and reactivity of sera to the peptide corresponding to HERG extracellular loop at the pore region.

Linear homology analysis showed that there is 44% homology between 52Ro protein (aa302-aa321) and HERG α_1 subunit (aa574-aa598) at the pore region (**Figure 8C-a,b,c**) of which 25% are identical. The presence of this homology at the pore region may account for anti-Ro Abs off target binding to HERG channel at this epitope mimic, especially in the tetrameric conformation model of the channel where the 4 pore extracellular loops come together and are accessible to the antibodies (**Figure 8C- c**)[26]. This was tested by performing ELISA using patients' sera and a synthesized 31 amino acid peptide corresponding to the pore-forming region of the HERG channel (**Figure 8C-a**). **Figure 8C-d** shows that anti-Ro Abs positive sera (n=3) but not anti-Ro Abs negative sera (n=3) exhibited high reactivity with the peptide. The average reactivity reading was 2.19±0.04 O.D. in anti-Ro Ab positive sera vs. 0.36±0.03 O.D in anti-Ro Ab negative sera; the difference was statistically significant (n=6, p<0.0001).

DOI: 10.1161/CIRCULATIONAHA.115.009800

Discussions

Here, we describe the pathogenesis underlying a novel form of acquired QT prolongation of autoimmune origin associated with anti-Ro Abs in adults. The in vitro data show that serum and purified IgG containing anti-Ro Abs as well as affinity purified anti-52Ro Abs from CTD patients with QTc prolongation, functionally inhibit I_{Kr} in a time and dose-dependent manner by direct interaction with the HERG/Kv11.1 channel protein. The in vivo data from guinea-pigs are first to establish an animal model whereby induction of anti-Ro Abs by immunization results in QTc prolongation on the ECG. Furthermore, using native cardiomyocytes, anti-Ro Ab positive IgG prolonged APD and inhibited I_{Kr} by directly interacting with the I_{Kr} channel likely at the pore region where homology between Ro antigen and HERG channel was identified and reactivity to anti-Ro Ab positive sera was observed.

Autoimmune associated electrical abnormalities in the clinical settings

The most well characterized autoimmune disease where anti-Ro Abs are associated with electrical abnormalities is congenital heart block (CHB) detected at or before birth in a structurally normal heart. [14, 27]. The hallmark of CHB is the irreversible complete AV block which affects exclusively the *fetus* and/or the *newborn* heart but curiously not the *adult* maternal heart despite exposure to the identical circulating anti-Ro Abs [14, 27]. QTc prolongation has also been reported in newborns[28, 29] of mothers with anti-Ro Abs but resolves over time with the disappearance of Abs[30] thus supporting the involvement of anti-Ro Abs in the pathogenesis of QTc prolongation. These findings impacted the 2002 guidelines of the European Society of Cardiology where close ECG monitoring of anti-Ro Ab positive neonates was proposed[31].

Recently, clinical evidence has demonstrated a correlation between the presence of anti-Ro Abs and QTc prolongation in adult patients with autoimmune diseases[7, 9, 10, 32]. Our

experimental findings support and are consistent with these clinical observations from different groups that the presence of anti-Ro Abs correlates with QTc prolongation[7-10, 32]. A study by Bourre-Tessier et al.[10], analyzing a large cohort of 278 patients affected with systemic lupus erythematosus found that the occurrence of QTc prolongation was about eightfold more likely in anti-Ro Abs positive than in negative patients. Similarly, Lazzerini et al, found that about half of anti-Ro/SSA-positive patients displayed a prolonged QTc[7, 9] and increased propensity for ventricular arrhythmias[9]. However, other studies did not show any significant differences in mean QTc likely because of the type of autoimmune disease studied, the age of the patients, the titers of Abs and the methods used for Abs analysis[33-35].

Animal model of autoimmune associated QTc prolongation

To correlate the arrhythmogenic effects of anti-Ro Abs with the genesis of QT interval prolongation, guinea-pigs were immunized with 52Ro antigen to generate anti-52Ro Abs. The data from this in vivo study are first to establish an animal model of autoimmune associated QTc prolongation and provide evidence for a pathogenic role of anti-52Ro Abs in the development of QTc prolongation. Moreover, anti-52Ro Abs positive but not negative sera from immunized guinea-pigs also inhibited I_{Kr} and cross-reacted with Kv11.1 channel protein. Together, along with the anti-Ro Ab positive IgG lengthening of APD in guinea-pig ventricular myocytes, these findings are consistent with the clinical observation that the sole presence of anti-Ro Abs correlates with QTc prolongation[7, 8, 10, 32].

Pathogenesis of autoimmune associated QTc prolongation

The proposed mechanism for the autoimmune associated QTc prolongation is that anti-Ro Abs cause APD and QTc prolongations by direct block of the HERG/Kv11.1 channels. Several line of evidence support this proposed mechanism: 1) only sera, IgG and affinity purified anti-Ro

Abs from anti-Ro Ab positive patients, but not anti-Ro negative patients, inhibited I_{Kr} and directly interacted with HERG/Kv11.1 channel proteins both in expression systems and in native ventricular myocytes; 2) anti-Ro Abs did not affect I_{Kr} kinetics and their effect was observed within minutes suggesting a direct block of the HERG channel; 3) the homology between 52Ro antigen and HERG channel at the pore forming region may account for anti-Ro Abs to target and block the pore of the HERG channel. This is supported by the tetrameric 3D model of the HERG pore region showing the accessibility of the extracellular loop between S5 and S6 to antibodies (**Figure 8C-c**) ; 4) the reactivity of anti-Ro Abs positive but not anti-Ro Abs negative sera with the peptide corresponding to the pore forming region of HERG; 5) the sole presence of anti-Ro Abs induced by immunization of guinea-pigs resulted in QTc prolongation on the surface ECG; 6) anti-Ro Abs do not affect other currents such as the delayed rectifier K current, I_{Ks} , the transient outward current, I_{to}, the inward rectifier K current, I_{K1} and the Na current, I_{Na}[36, 37].

Because it is generally accepted that QT interval is a function of ventricular AP duration and that the two variables are very closely correlated in Humans [38, 39] and animals [40], the combined in vitro and in vivo data from this study provided important clues on the relationship between ion channel block, APD lengthening and QT interval prolongation. Abnormal QTc interval prolongation is known to predispose to ventricular arrhythmias known as Torsade de Pointes via early afterdepolarization induced triggered activity. Thus, anti-Ro Ab induced QTc prolongation confers an increased risk of ventricular arrhythmias not only for patients with anti-Ro Abs but also for patients with genetic and/or drug induced QTc prolongation. In fact, anti-Ro Ab is the most frequent autoantibody found in the general population (up to about 3%), but anti-Ro Ab positive patients are in most cases asymptomatic for autoimmune diseases[41]. The involvement of anti-Ro Abs and HERG channel in the pathogenesis of QTc prolongation is

further supported by a case report where I_{Kr} has been shown to be inhibited by anti-Ro Abs from a female patient (asymptomatic for autoimmune diseases) with an acquired long QT syndrome with no known cause of QTc prolongation except for positive anti-Ro Abs [42]. Altogether, both clinical and experimental evidences support the association of anti-Ro Abs with QTc prolongation in adult patients and pinpoint to anti-Ro Abs' inhibition of the HERG/Kv11.1 channel as a plausible underlying mechanism.

Significance

Patients with QTc prolongation are prone to complex ventricular arrhythmias including Torsade de Pointes, syncope and sudden death[3, 4]. QTc prolongation associated with anti-Ro Abs *per se* may confer an increased risk for developing ventricular arrhythmias and represents an additional risk factor for patients with drug induced or congenital QTc prolongation. The finding from the present study supports the recommendation that adult patients with anti-Ro Abs may benefit from routine ECG screening for QTc prolongation and those already identified with anti-Ro Ab associated QTc prolongation should receive counseling, including education about avoiding drugs and other conditions known to prolong the QT interval.

Funding Sources: The work was supported by Award Number I01BX007080 from Biomedical Laboratory Research & Development Service of Veterans Affairs Office of Research and Development.

Conflict of Interest Disclosures: None.

References:

1. Roden DM. Cellular basis of drug-induced torsades de pointes. *Br J Pharmacol*. 2008;154:1502-1507.

2. Schwartz PJ, Periti M, Malliani A. The long Q-T syndrome. *Am Heart J*. 1975;89:378-390.

3. Farkas AS, Nattel S. Minimizing repolarization-related proarrhythmic risk in drug development and clinical practice. *Drugs*. 2010;70:573-603.

4. Keating MT, Sanguinetti MC. Molecular and cellular mechanisms of cardiac arrhythmias. *Cell*. 2001;104:569-580.

5. Kannankeril P, Roden DM, Darbar D. Drug-induced long QT syndrome. *Pharmacol Rev*. 2010;62:760-781.

6. Roden DM, Abraham RL. Refining repolarization reserve. *Heart Rhythm*. 2011;8:1756-1757.

7. Lazzerini PE, Acampa M, Guideri F, Capecchi PL, Campanella V, Morozzi G, Galeazzi M, Marcolongo R, Laghi-Pasini F. Prolongation of the corrected QT interval in adult patients with anti-Ro/SSA-positive connective tissue diseases. *Arthritis Rheum*. 2004;50:1248-1252.

8. Lazzerini PE, Capecchi PL, Guideri F, Acampa M, Selvi E, Bisogno S, Galeazzi M, Laghi-Pasini F. Autoantibody-mediated cardiac arrhythmias: mechanisms and clinical implications. *Basic Res Cardiol*. 2008;103:1-11.

9. Lazzerini PE, Capecchi PL, Guideri F, Bellisai F, Selvi E, Acampa M, Costa A, Maggio R, Garcia-Gonzalez E, Bisogno S, Morozzi G, Galeazzi M, Laghi-Pasini F. Comparison of frequency of complex ventricular arrhythmias in patients with positive versus negative anti-Ro/SSA and connective tissue disease. *Am J Cardiol*. 2007;100:1029-1034.

10. Bourre-Tessier J, Clarke AE, Huynh T, Bernatsky S, Joseph L, Belisle P, Pineau CA. Prolonged corrected QT interval in anti-Ro/SSA-positive adults with systemic lupus erythematosus. *Arthritis Care Res (Hoboken)*. 2011;63:1031-1037.

11. Franceschini F, Cavazzana I. Anti-Ro/SSA and La/SSB antibodies. *Autoimmunity*. 2005;38:55-63.

12. Lazzerini PE, Capecchi PL, Laghi-Pasini F. Anti-Ro/SSA antibodies and cardiac arrhythmias in the adult: facts and hypotheses. *Scand J Immunol*. 2010;72:213-222.

13. Buyon JP, Clancy RM, Friedman DM. Autoimmune associated congenital heart block: integration of clinical and research clues in the management of the maternal / foetal dyad at risk. *J Intern Med*. 2009;265:653-662.

14. Qu Y, Boutjdir M. Pathophysiology of Autoimmune Associated Congenital Heart Block. From *Prediction to Prevention of Autoimmune Diseases.* K Conrad, KL Chan, MJ Fritzler, RL Humbel, Y Shoenfeld (Eds). 2011;17:289-310.

15. Rautaharju PM, Surawicz B, Gettes LS, Bailey JJ, Childers R, Deal BJ, Gorgels A, Hancock EW, Josephson M, Kligfield P, Kors JA, Macfarlane P, Mason JW, Mirvis DM, Okin P, Pahlm O, van Herpen G, Wagner GS, Wellens H. AHA/ACCF/HRS recommendations for the standardization and interpretation of the electrocardiogram: part IV: the ST segment, T and U

waves, and the QT interval: a scientific statement from the American Heart Association Electrocardiography and Arrhythmias Committee, Council on Clinical Cardiology; the American College of Cardiology Foundation; and the Heart Rhythm Society. Endorsed by the International Society for Computerized Electrocardiology. *J Am Coll Cardiol*. 2009;53:982-991.

16. Boutjdir M, Chen L, Zhang ZH, Tseng CE, DiDonato F, Rashbaum W, Morris A, el-Sherif N, Buyon JP. Arrhythmogenicity of IgG and anti-52-kD SSA/Ro affinity-purified antibodies from mothers of children with congenital heart block. *Circ Res*. 1997;80:354-362.

17. Espinosa A, Hennig J, Ambrosi A, Anandapadmanaban M, Abelius MS, Sheng Y, Nyberg F, Arrowsmith CH, Sunnerhagen M, Wahren-Herlenius M. Anti-Ro52 autoantibodies from patients with Sjogren's syndrome inhibit the Ro52 E3 ligase activity by blocking the E3/E2 interface. *J Biol Chem*. 2011;286:36478-36491.

18. Zhou Z, Gong Q, Ye B, Fan Z, Makielski JC, Robertson GA, January CT. Properties of HERG channels stably expressed in HEK 293 cells studied at physiological temperature. *Biophys J*. 1998;74:230-241.

19. Drolet B, Vincent F, Rail J, Chahine M, Deschenes D, Nadeau S, Khalifa M, Hamelin BA, Turgeon J. Thioridazine lengthens repolarization of cardiac ventricular myocytes by blocking the delayed rectifier potassium current. *J Pharmacol Exp Ther*. 1999;288:1261-1268.

20. Miranda-Carus ME, Boutjdir M, Tseng CE, DiDonato F, Chan EK, Buyon JP. Induction of antibodies reactive with SSA/Ro-SSB/La and development of congenital heart block in a murine model. *J Immunol*. 1998;161:5886-5892.

21. Karnabi E, Qu Y, Mancarella S, Boutjdir M. Rescue and worsening of congenital heart block-associated electrocardiographic abnormalities in two transgenic mice. *J Cardiovasc Electrophysiol*. 2011;22:922-930.

22. Xiao GQ, Qu Y, Hu K, Boutjdir M. Down-regulation of L-type calcium channel in pups born to 52 kDa SSA/Ro immunized rabbits. *FASEB J*. 2001;15:1539-1545.

23. Zhou Z, Gong Q, Epstein ML, January CT. HERG channel dysfunction in human long QT syndrome. Intracellular transport and functional defects. *J Biol Chem*. 1998;273:21061-21066.

24. Hamlin RL, Kijtawornrat A, Keene BW, Hamlin DM. QT and RR intervals in conscious and anesthetized guinea pigs with highly varying RR intervals and given QTc-lengthening test articles. *Toxicol Sci*. 2003;76:437-442.

25. Shiotani M, Harada T, Abe J, Hamada Y, Horii I. Methodological validation of an existing telemetry system for QT evaluation in conscious guinea pigs. *J Pharmacol Toxicol Methods*. 2007;55:27-34.

26. Wynia-Smith SL, Gillian-Daniel AL, Satyshur KA, Robertson GA. hERG gating microdomains defined by S6 mutagenesis and molecular modeling. *J Gen Physiol*. 2008;132:507-520.

27. Buyon JP, Clancy RM, Friedman DM. Cardiac manifestations of neonatal lupus erythematosus: guidelines to management, integrating clues from the bench and bedside. *Nat Clin Pract Rheumatol*. 2009;5:139-148.

28. Cimaz R, Stramba-Badiale M, Brucato A, Catelli L, Panzeri P, Meroni PL. QT interval prolongation in asymptomatic anti-SSA/Ro-positive infants without congenital heart block. *Arthritis Rheum*. 2000;43:1049-1053.

29. Gordon PA, Khamashta MA, Hughes GR, Rosenthal E. Increase in the heart rate-corrected QT interval in children of anti-Ro-positive mothers, with a further increase in those with siblings with congenital heart block: comment on the article by Cimaz et al. *Arthritis Rheum*. 2001;44:242-243.

30. Cimaz R, Meroni PL, Brucato A, Fesstova V, Panzeri P, Goulene K, Stramba-Badiale M. Concomitant disappearance of electrocardiographic abnormalities and of acquired maternal autoantibodies during the first year of life in infants who had QT interval prolongation and anti-SSA/Ro positivity without congenital heart block at birth. *Arthritis Rheum*. 2003;48:266-268.

31. Schwartz PJ, Garson A, Jr., Paul T, Stramba-Badiale M, Vetter VL, Wren C, European Society of C. Guidelines for the interpretation of the neonatal electrocardiogram. A task force of the European Society of Cardiology. *Eur Heart J*. 2002;23:1329-1344.

32. Lazzerini PE, Capecchi PL, Acampa M, Morozzi G, Bellisai F, Bacarelli MR, Dragoni S, Fineschi I, Simpatico A, Galeazzi M, Laghi-Pasini F. Anti-Ro/SSA-associated corrected QT interval prolongation in adults: the role of antibody level and specificity. *Arthritis Care Res (Hoboken)*. 3010;63:1463-1470.

33. Costedoat-Chalumeau N, Amoura Z, Hulot JS, Ghillani P, Lechat P, Funck-Brentano C, Piette JC. Corrected QT interval in anti-SSA-positive adults with connective tissue disease: comment on the article by Lazzerini et al. *Arthritis Rheum*. 2005;52:676-677; author reply 677-8.

34. Gordon PA, Rosenthal E, Khamashta MA, Hughes GR. Absence of conduction defects in the electrocardiograms [correction of echocardiograms] of mothers with children with congenital complete heart block. *J Rheumatol*. 2001;28:366-369.

35. Bourre-Tessier J, Urowitz MB, Clarke AE, Bernatsky S, Krantz MJ, Huynh T, Joseph L, Belisle P, Bae SC, Hanly JG, Wallace DJ, Gordon C, Isenberg D, Rahman A, Gladman DD, Fortin PR, Merrill JT, Romero-Diaz J, Sanchez-Guerrero J, Fessler B, Alarcon GS, Steinsson K, Bruce IN, Ginzler E, Dooley MA, Nived O, Sturfelt G, Kalunian K, Ramos-Casals M, Petri M, Zoma A, Pineau CA. Electrocardiographic findings in systemic lupus erythematosus: data from an international inception cohort. *Arthritis Care Res (Hoboken)*. 2015;67:128-135.

36. Xiao GQ, Hu K, Boutjdir M. Direct inhibition of expressed cardiac l- and t-type calcium channels by igg from mothers whose children have congenital heart block. *Circulation*. 2001;103:1599-1604.

37. Boutjdir M, Chen L, Zhang ZH, Tseng CE, El-Sherif N, Buyon JP. Serum and immunoglobulin

G from the mother of a child with congenital heart block induce conduction abnormalities and inhibit L-type calcium channels in a rat heart model. *Pediatr Res*. 1998;44:11-19.

38. Seed WA, Noble MI, Oldershaw P, Wanless RB, Drake-Holland AJ, Redwood D, Pugh S, Mills C. Relation of human cardiac action potential duration to the interval between beats: implications for the validity of rate corrected QT interval (QTc). *Br Heart J*. 1987;57:32-37.

39. Yan GX, Lankipalli RS, Burke JF, Musco S, Kowey PR. Ventricular repolarization components on the electrocardiogram: cellular basis and clinical significance. *J Am Coll Cardiol*. 2003;42:401-409.

40. Yan GX, Antzelevitch C. Cellular basis for the normal T wave and the electrocardiographic manifestations of the long-QT syndrome. *Circulation*. 1998;98:1928-1936.

41. Hayashi N, Koshiba M, Nishimura K, Sugiyama D, Nakamura T, Morinobu S, Kawano S, Kumagai S. Prevalence of disease-specific antinuclear antibodies in general population: estimates from annual physical examinations of residents of a small town over a 5-year period. *Mod Rheumatol*. 2008;18:153-160.

42. Nakamura K, Katayama Y, Kusano KF, Haraoka K, Tani Y, Nagase S, Morita H, Miura D, Fujimoto Y, Furukawa T, Ueda K, Aizawa Y, Kimura A, Kurachi Y, Ohe T. Anti-KCNH2 antibody-induced long QT syndrome: novel acquired form of long QT syndrome. *J Am Coll Cardiol*. 2007;50:1808-1809.

Table 1. Clinical characteristics of patients studied.

Serum/Patients	Gender	Age	CTD diagnosis	QTc (ms)
Anti-Ro antibody positive				
#1	F	35	SS	566
#2	F	37	SS	514
#3	F	42	SS	498
Anti-Ro antibody negative				
#4	M	65	SS	404
#5	M	23	SLE	451
#6	F	31	SLE	430

CTD: Connective tissue disease; SS: Sjögren's Syndrome; SLE: Systemic lupus erythematosus; F: Female; M: Male. QTc: Corrected QT interval.

Table 2. Electrocardiogram parameters and antibody levels before and after immunization.

	QTc (ms)	Heart Rate (bpm)	PR Interval (ms)	QRS (ms)	Anti-Ro Antibodies Range (O.D)
Baseline (n=7)	248.3±30	294.4±12	50.5±2.9	19.1±1.0	0.02-0.04
Immunized (n=7)	272.5±23*	280.2±42	56.5±1.4	19.2±2.0	1.14-2.16*

QTc: Corrected QT interval; bpm: beat per minutes; O.D: Optical Density; *p<0.05.

DOI: 10.1161/CIRCULATIONAHA.115.009800

Figure Legends:

Figure 1. Anti-Ro Ab positive sera inhibits I_{Kr}. (A) Twelve lead ECG of patient #1 who is anti-Ro Ab positive and has a long QTc of 566 ms. Vertical lines in lead II show QT interval. (B) Protocol used to record I_{Kr} currents from HEK293 cells stably expressing HERG channels. I_{Kr} peak was elicited by 4-sec depolarizing pulses in 10 mV steps from -60 mV to 60 mV from a holding potential of -80 mV. I_{Kr} tail was recorded upon repolarization to -50 mV for 5 sec. (C) Representative current traces under basal conditions and (D) in the presence of serum #1 (200 µl). I-V relationships of I_{Kr} peak (E) and tail (F) densities during basal (circles) and anti-Ro Ab positive serum #1 application (triangles). (G) Summary dot plot of the inhibition of I_{Kr} peak and tail densities at -10 mV by anti-Ro Ab positive sera from three different patients with QTc prolongation (>460 ms) and connective tissue disease. (∗) Indicates statistical significance at $p<0.05$ (n=10 each).

Figure 2. Anti-Ro Ab negative sera has no effect on I_{Kr}. (A) Twelve lead ECG of a control patient #4 who is anti-Ro Ab negative and has a normal QTc of 404 ms. Vertical lines in lead II show QT interval. Currents were recorded from HEK293 stably expressing HERG channels using the protocol shown in Figure 1B. (B) I_{Kr} current traces during basal conditions and (C) in the presence of anti-Ro Ab negative serum (200 µl). I-V relationships during basal conditions (circles) and anti-Ro Ab negative serum (triangles) for I_{Kr} peak (D) and tail (E). (F) Summary dot plot of I_{Kr} peak and tail densities in the presence of anti-Ro Ab negative sera from three different patients with normal QTc (<460 ms) and connective tissue disease.

DOI: 10.1161/CIRCULATIONAHA.115.009800

Figure 3. Anti-Ro Ab positive IgG purified from serum #1 inhibits I_{Kr}. Currents were recorded from HEK293 stably expressing HERG channels using the protocol shown in panel B of Figure 1. (A) Representative current traces under basal conditions and (B) in the presence of 75 µg/ml anti-Ro Ab positive IgG. I-V relationships of I_{Kr} peak (C) and tail (D) current densities during basal (circles) and anti-Ro positive IgG application (triangles). The corresponding dot plot at -10 mV is shown in (E) for I_{Kr} peak and I_{Kr} tail densities before and after IgG. (*) Indicates statistical significance at $p<0.05$ ($n=10$).

Figure 4. Dose- and time-dependent effects of IgG on HERG I_{Kr} and its kinetics. (A) Dose-response curve of anti-Ro positive IgG ($n=6$) resulted in an EC_{50}=87.3 µg/ml. (B) Time course of anti-Ro Abs positive IgG (75 µg/ml) from serum #1 on I_{Kr} peak. (C) Time course of anti-Ro Abs negative IgG (75 µg/ml) from serum #4 of a control patient on I_{Kr} peak. (D) Time course of I_{Kr} peak rundown. (E) and (F) illustrate the Boltzmann fit of I_{Kr} activation and deactivation before (circle) and after anti-Ro Abs positive IgG application (triangle). The dashed lines indicate the time of IgG application and washout as indicated.

Figure 5. Anti-Ro Abs positive IgG cross-react with HERG channel. (A) Proteins from un-transfected (lane 1) and transfected HEK293 cells with HERG channels (lane 2) were probed with anti-Ro Ab positive IgG from serum #1. Bands at 155 kDa and 135 kDa correspond to glycosylated and endoplasmic reticulum-retained HERG channels in lane 2 only. (B) Proteins from un-transfected (lane 3) and transfected HEK293 cells with HERG channels (lane 4) where probed with anti-Ro Ab negative IgG from serum #4. (C) Proteins from un-transfected (lane 5) and transfected HEK293 cells with HERG channels (lane 6) were probed with a commercial

anti-HERG channel Ab. Bands at 155 kDa and 135 kDa were seen in lane 6 only as in lane 2 with anti-Ro Ab positive IgG. The 37 kDa bands represents GAPDH.

Figure 6. Affinity purified anti-52kDa Ro Abs inhibit I_{Kr}. Currents were recorded from HEK293 stably expressing HERG channels using the protocol shown in Figure 1B. (A) Representative current traces under basal conditions and (B) in the presence of 52 μg/ml affinity purified anti-52Ro Ab from sera #1. I-V relationships of I_{Kr} peak (C) and tail (D) densities during basal (circles) and affinity purified anti-Ro Abs application (triangles). The corresponding dot plot at -10 mV is shown in (E) for I_{Kr} peak and for I_{Kr} tail density before and after IgG. (*) Indicates statistical significance at $p<0.05$ ($n=10$).

Figure 7. In vivo and in vitro effects of anti-Ro Abs in guinea-pigs. Representative ECGs from a guinea-pig (A) before immunization and (B) after immunization with 52Ro antigen. Vertical lines indicate QT interval. (C) Effects of anti-Ro Ab positive IgG from serum #1 on action potential duration and (D) on I_{Kr} current recorded from guinea-pig ventricular myocytes. Averaged data from 6 experiments each for anti-Ro Ab positive and negative are presented in the dot plot. (E) Shows Western blots of anti-Ro Ab positive IgG (left panel) on un-transfected HEK293 cells (lane 1), HEK293 cells expressing HERG channel (lane 2) and guinea-pig ventricular tissue (lane 3). Additional positive controls with HEK293 cells expressing HERG channel and guinea-pig ventricular tissue are shown respectively in lanes 5 and 6 and negative control with un-transfected HEH293 cells (lane 4). (*) Indicates statistical significance at $p<0.05$.

Figure 8. Effects of guinea-pig sera on I_{Kr}, homology comparison and sera reactivity to the

DOI: 10.1161/CIRCULATIONAHA.115.009800

peptide corresponding to the pore forming region of HERG channel. Representative I_{Kr} tracings (A) before (left) and after (right) the application of anti-Ro Ab positive serum from an immunized guinea-pig. (B) Western blot of guinea-pig ventricles probed with anti-Ro Ab positive (lane 1) and anti-Ro Ab negative (lane 2) guinea-pig sera. (C-a) Schematic representation of the secondary structure of a single HERG channel α_1-subunit. The six segments (S1–S6) are shown along with the intracellularly located N- and C-termini. The pore forming extracellular loop is located between S5 and S6 where single and double circles illustrate similar and identical amino acids (aa) between 52Ro protein and HERG channel, respectively. (C-b) Linear homology analysis between 52Ro protein and HERG channel at the pore region. (C-c) Tetrameric structure of HERG channel model at the pore region based on KcsA crystal structure. Left panel shows the top view and right panel the front view of the pore region. Red represents segment S5/S6 helices and blue the predicted anti-Ro Ab binding sites in the extracellular loop between S5/S6 based on the homology shown in C-b. (C-d) Reactivity of patient's sera to the peptide corresponding to the pore forming region of HERG.

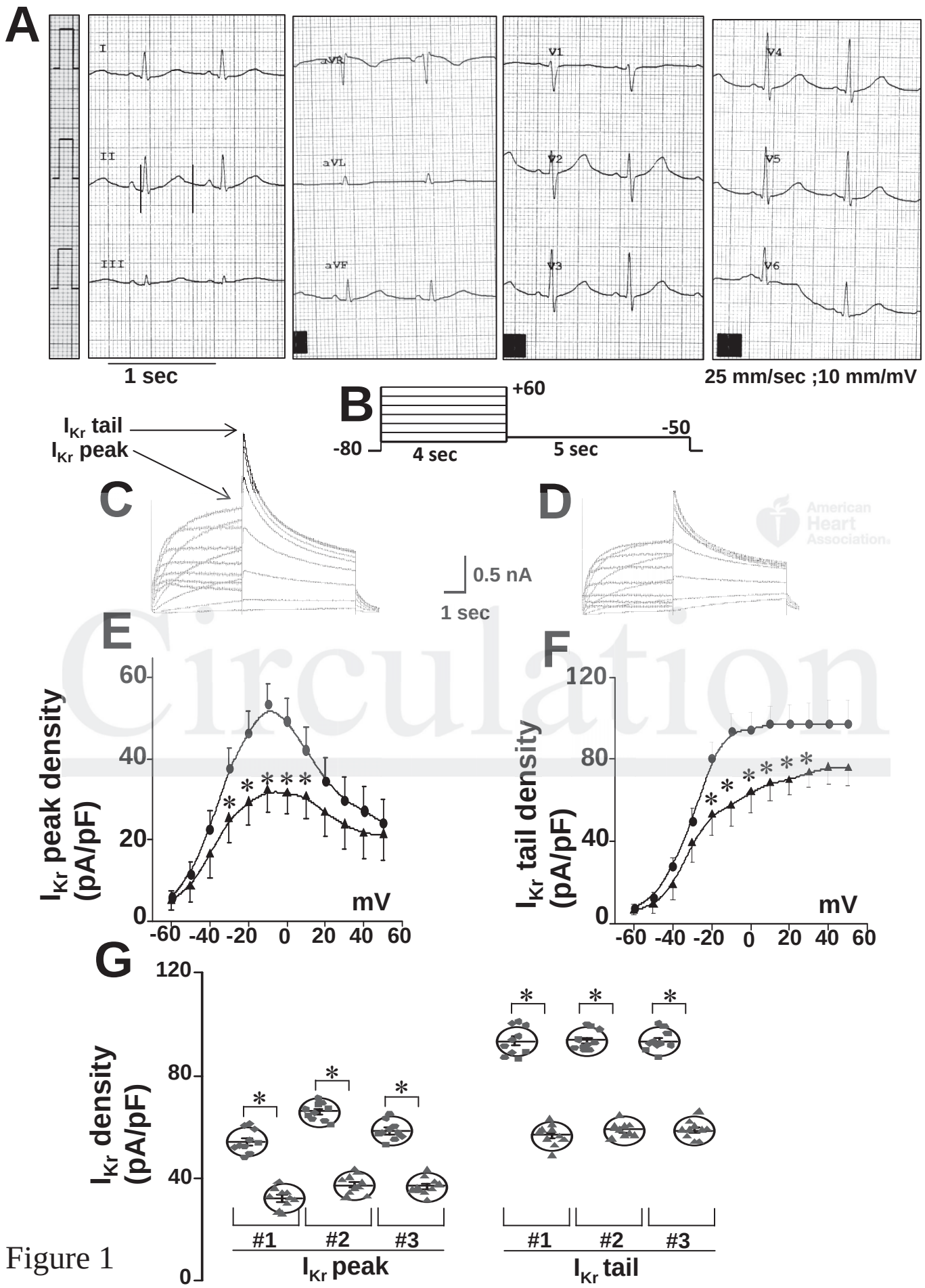

Figure 1

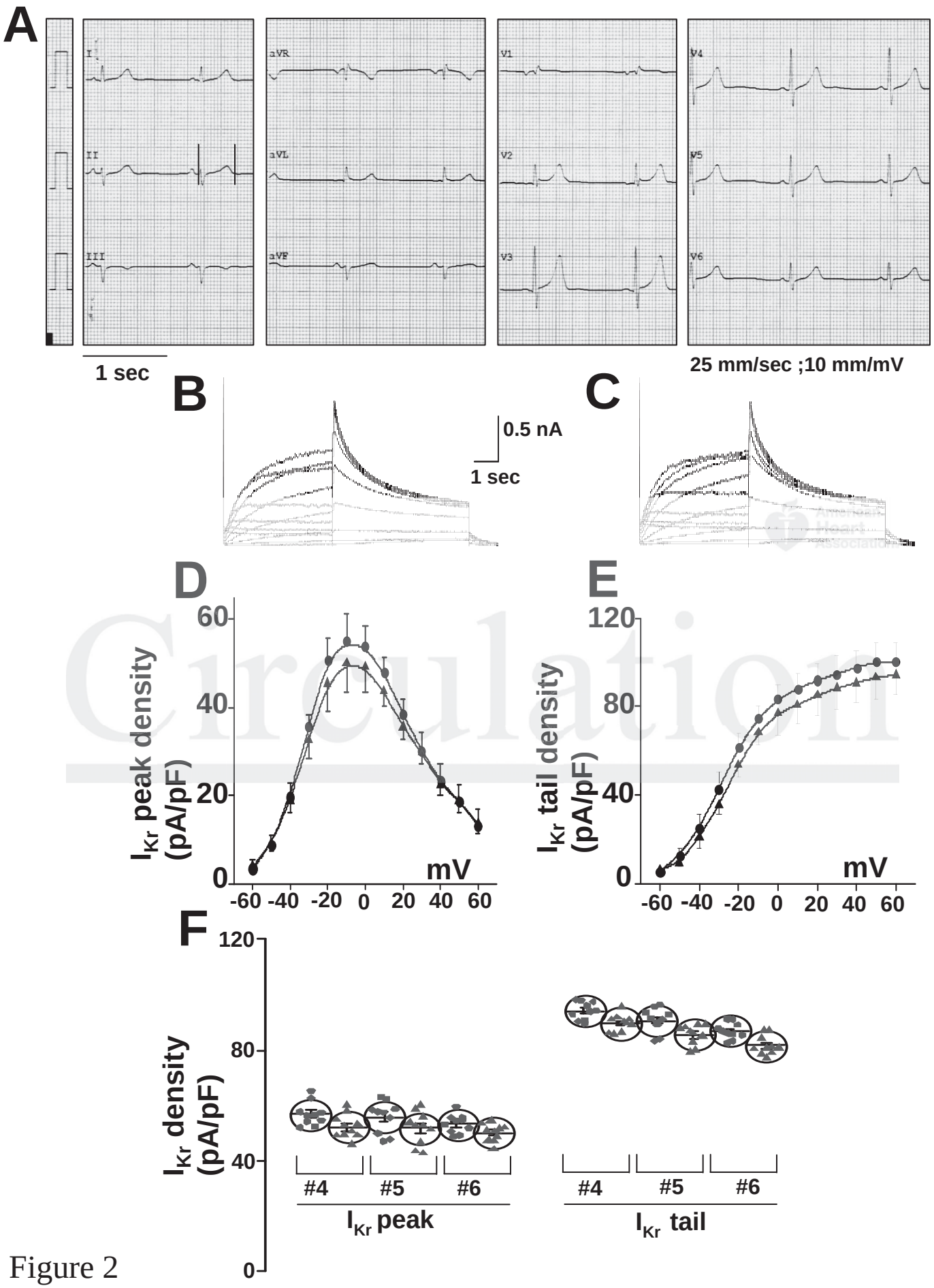

Figure 2

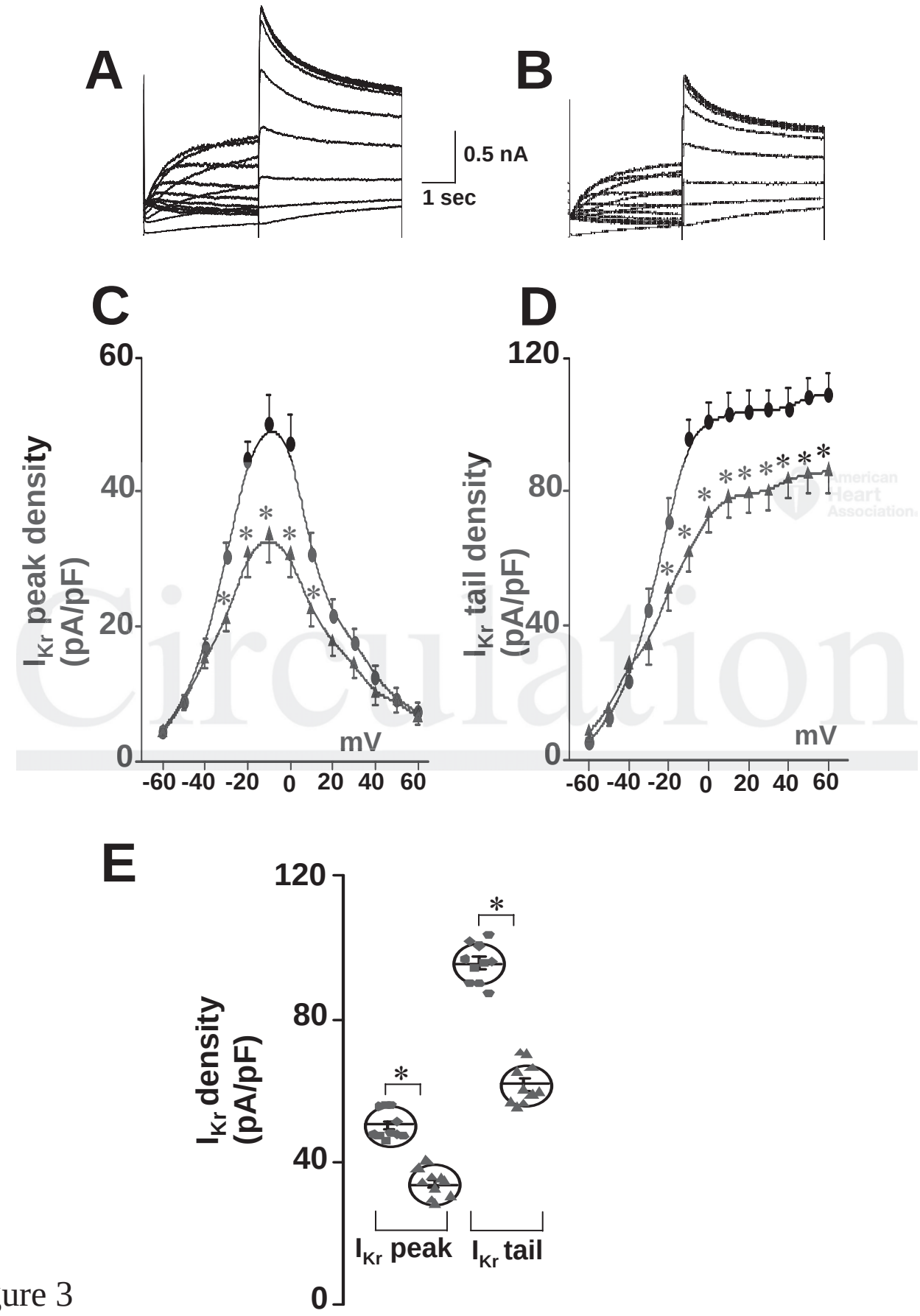

Figure 3

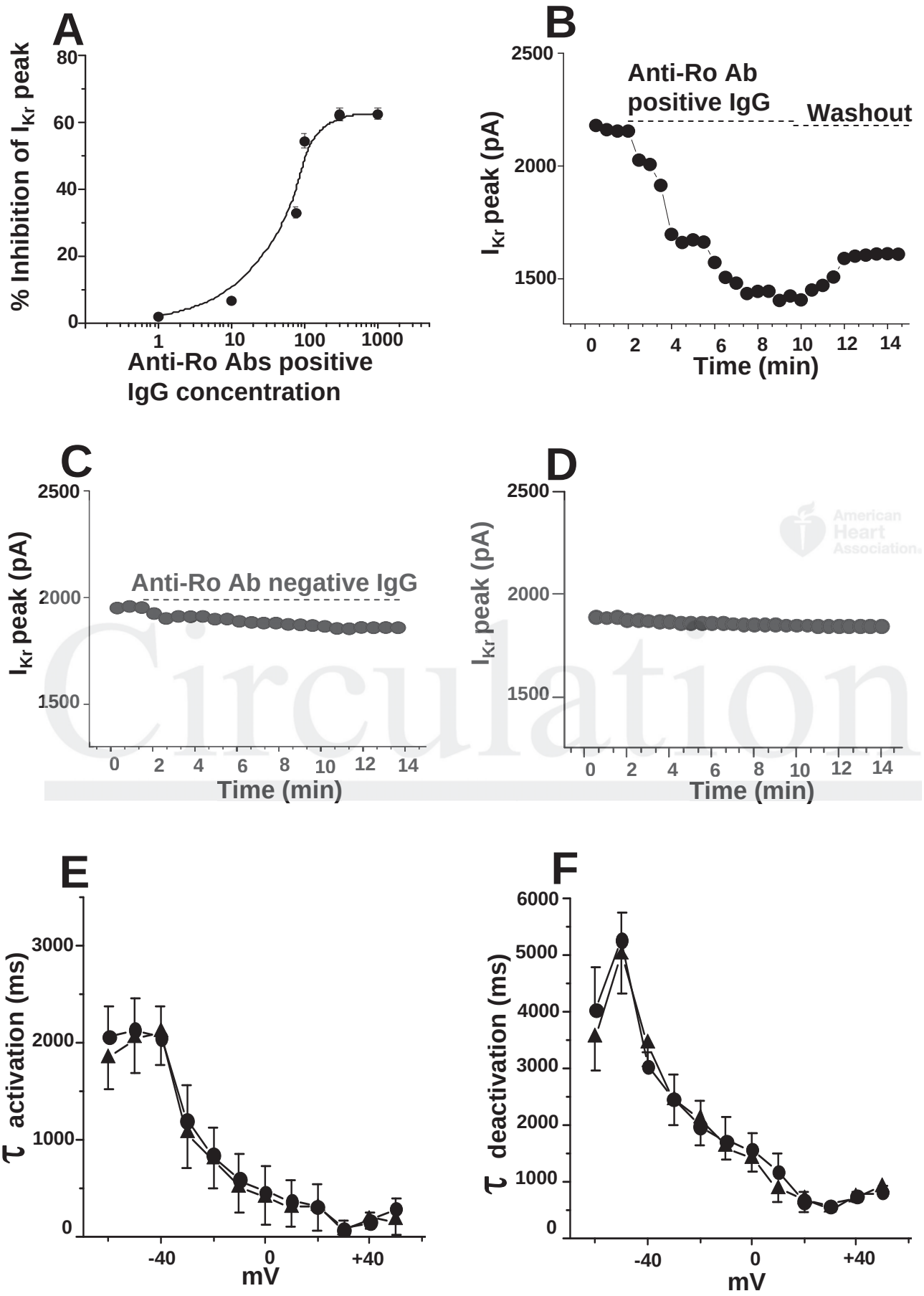

Figure 4

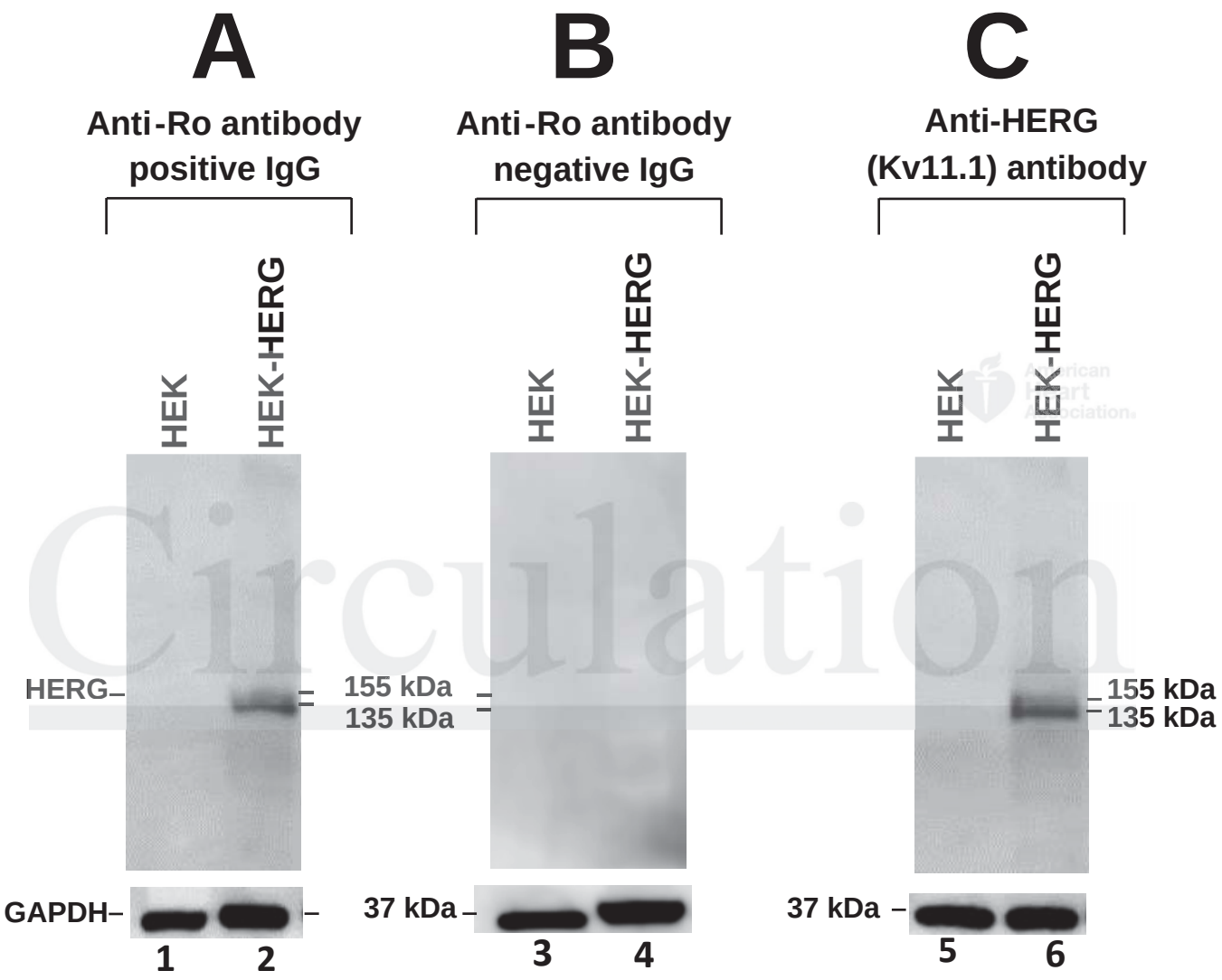

Figure 5

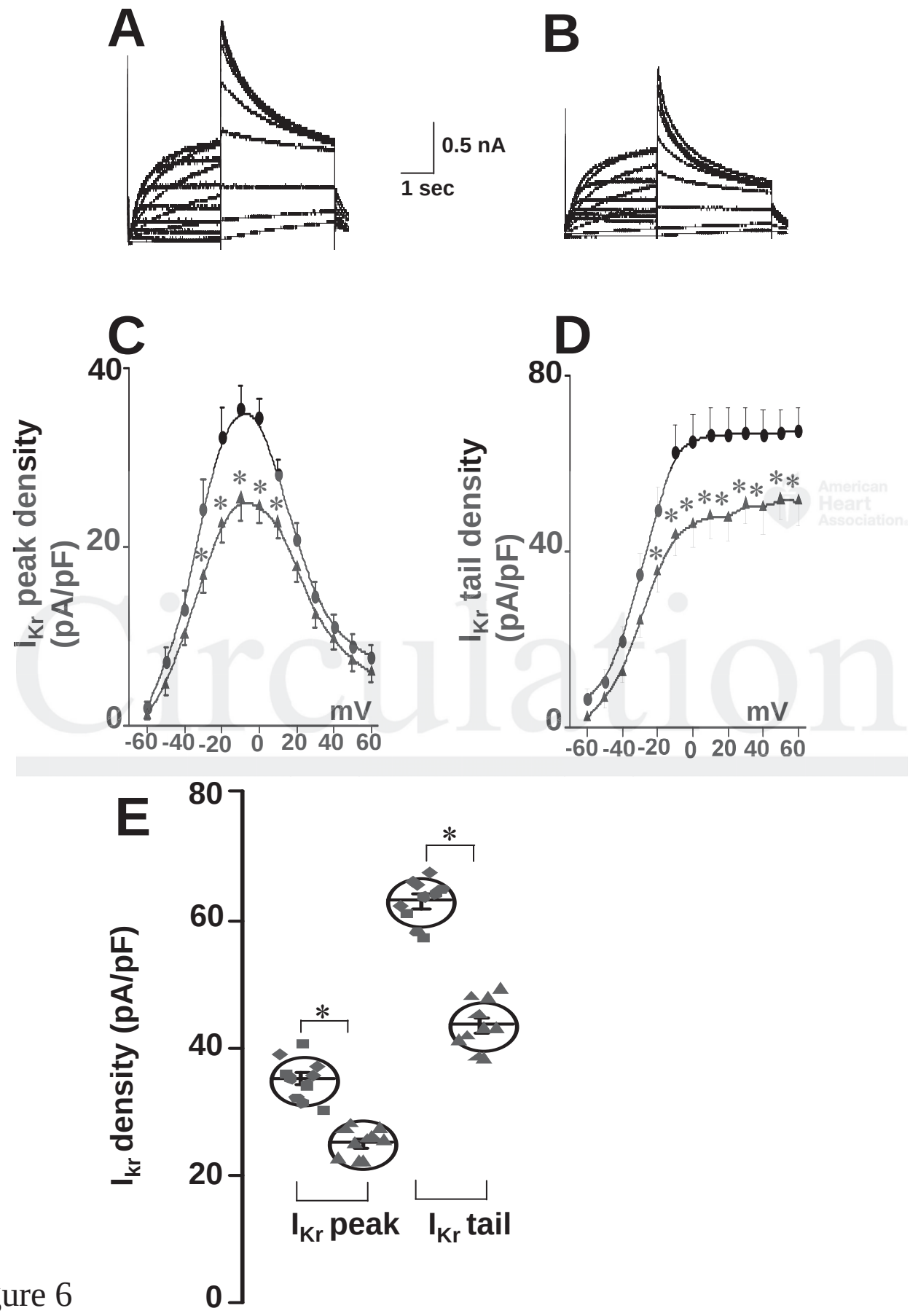

Figure 6

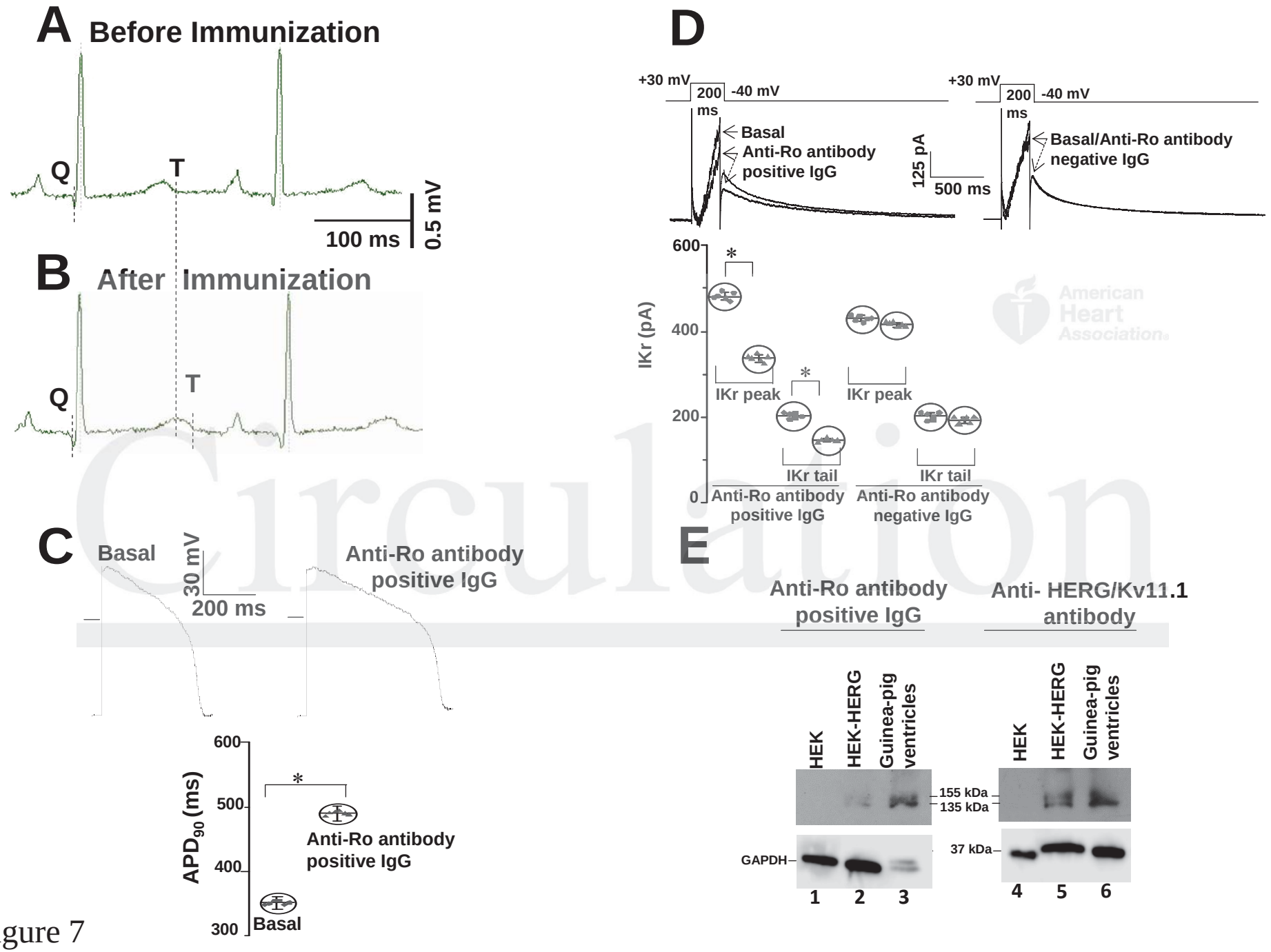

Figure 7

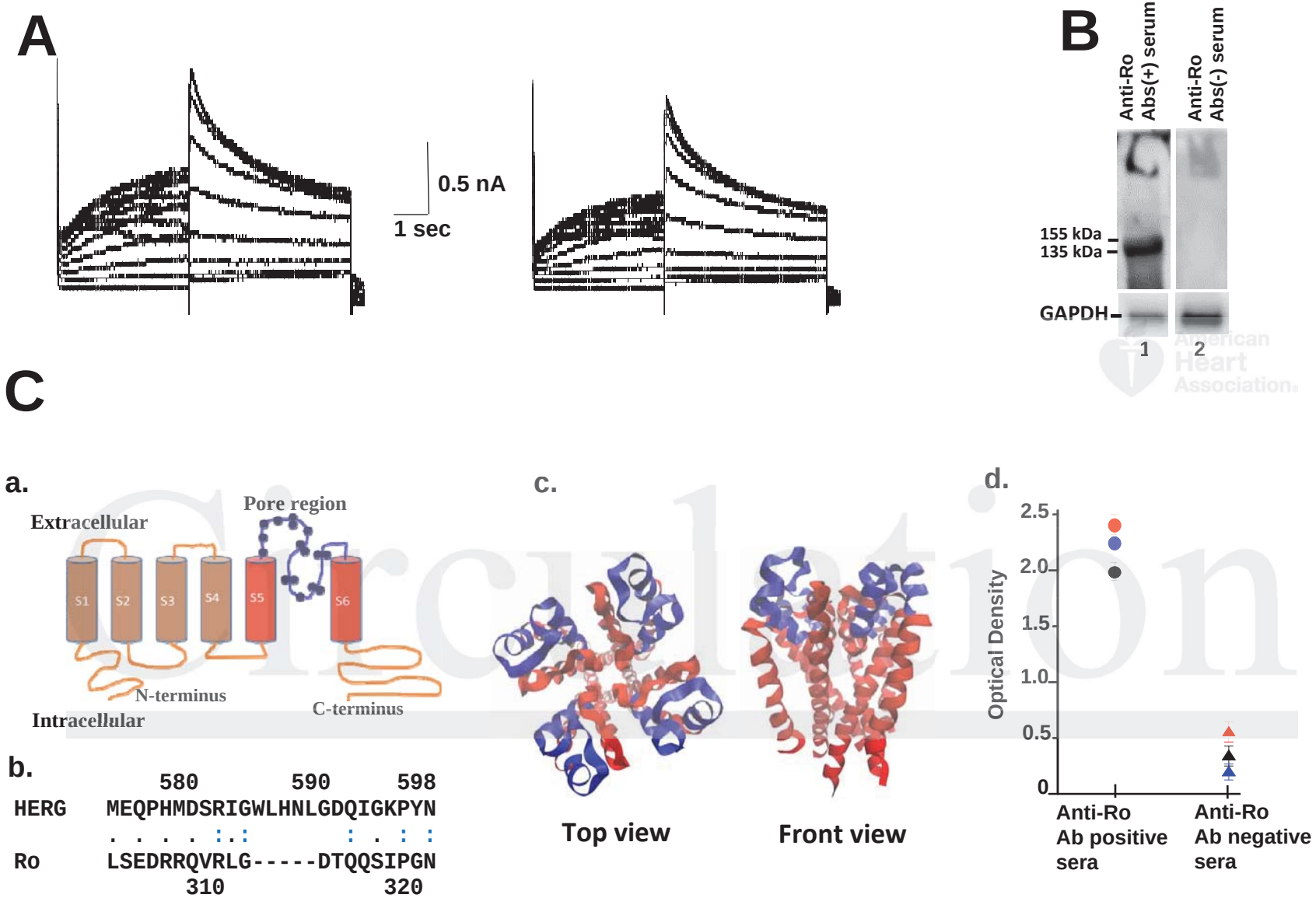

Figure 8

Pathogenesis of the Novel Autoimmune-Associated Long QT Syndrome

Yuankun Yue, Monica Castrichini, Ujala Srivastava, Frank Fabris, Krupa Shah, Zhiqiang Li, Yongxia Qu, Nabil El-Sherif, Zhengfeng Zhou, Craig January, M. Mahmood Hussain, Xian-Cheng Jiang, Eric A. Sobie, Marie Wahren-Herlenius, Mohamed Chahine, Pier-Leopoldo Capecchi, Franco Laghi-Pasini, Pietro-Enea Lazzerini and Mohamed Boutjdir

Circulation. published online May 20, 2015;
Circulation is published by the American Heart Association, 7272 Greenville Avenue, Dallas, TX 75231

Print ISSN: 0009-7322. Online ISSN: 1524-4539

Supplemental Methods

ECG recordings in patients: In this study, QTc was considered prolonged if ≥460 ms in accordance with the AHA/ACC/HRS recommendations[1]. QT interval was manually measured on a 12-lead ECG from the onset of the Q wave or the onset of the QRS complex to the end of the T wave, defined as the return to the T-P baseline. When U waves are present, the QT interval was measured to the nadir of the curve between the T and U waves. QT interval, determined as the longest measured QT interval in any lead, was corrected for heart rate by Bazett's formula (dividing the QT interval by the square root of the R-R interval) to yield the QTc value. QTc is measured by a single investigator who was blinded to the patient's Abs status.

Purification of IgG and affinity purification of anti-52kDa/Ro antibodies from patients' sera: IgG purification was performed using Melon Gel IgG spin purification Kit (Thermo scientific). Briefly, 10-100 μL of serum per 100 μL of settled gel was used and the Melon Gel IgG purification support and purification buffer was equilibrated to room temperature. To obtain an even suspension, bottle containing the purification support was swirled and a 500 μL of slurry and dispensed into a spin column placed in a micro centrifuge tube. The uncapped column/tube assembly was centrifuged at 2,000-6,000 ×g for 1 minute. Purification buffer (300 μL) was added to the column, pulse centrifuged for 10 seconds and flow through discarded. 100-500 μL of diluted or 10-100 μL of buffer-exchanged serum was added to the column and incubated for 5 minutes at room temperature with end-over-end mixing. Centrifugation for 1 minute was performed to collect the purified Ab. For affinity purification of anti-52kDa Ro (52Ro) Abs, purified 52Ro protein was separated by 4-15% SDS-PAGE. The protein was transferred to nitrocellulose membrane and membrane areas with bound 52Ro protein were identified by immunoblotting. The membrane was blocked in 5% fat free milk in PBS-Tween (0.05%) for 30

minutes to prevent non-specific binding. Membrane areas with bound 52Ro were then excised and incubated overnight at 4°C in patient serum at a 1:10 dilution in PBS-Tween. The membrane was then washed thrice in PBS-Tween for 5 minutes each and the bound anti-52Ro Abs were eluted by incubating membrane in 0.1M Glycine (pH 2.8). Tris (1M) pH 9 was added in a 10:1 ratio to neutralize the pH of the final solution with anti-52Ro Abs.

Electrophysiology

HEK293 cells stably expressing HERG channel: The stably transfected cells were cultured in minimum essential medium (MEM) supplemented with 10% fetal bovine serum and 400 µg/ml geneticin (G418). For electrophysiological studies, cells were washed twice with standard MEM medium, and stored in this medium at room temperature for later use. Cells were superfused with HEPES-buffered Tyrode's solution containing (in mM): 137 NaCl, 4 KCl, 1.8 $CaCl_2$, 1 $MgCl_2$, 10 glucose, and 10 HEPES (pH 7.4 with NaOH). The internal pipette solution contained (in mM): 130 KCl, 1 $MgCl_2$, 5 EGTA, 5 MgATP, 10 HEPES (pH 7.2 with KOH). IKr was recorded using a standard protocol shown in Figure 1B. IKr kinetics were studied by fitting the activation and deactivation of IKr using Boltzmann equation as previously reported[2]. Experiments were performed at room temperature.

Guinea-pig ventricular myocytes: All experiments were performed in accordance with the IACUC at the VA New York Harbor Healthcare System and conform to the NIH guidelines. Guinea pigs were anesthetized with isoflurane and the heart was rapidly excised and Langendorff perfused with the following Tyrode's solution (in mM): 140 NaCl, 4.5 KCl, 2 $CaCl_2$, 10 dextrose, 1 $MgCl_2$, and 10 HEPES (pH = 7.4) for 2 min. The heart was then perfused with a Ca-free Tyrode's solution followed by collagenase B (final concentration, 1mg/ml; Boehringer Mannheim, Indianapolis, IN). The dispersed cells were resuspended in KB solution and

maintained at room temperature before use. The external solution used for IKr recordings contained (in mM): 145 NaCl, 4.5 KCl, 1 $MgCl_2$, 1.8 $CaCl_2$, 10 HEPES, and 10 glucose (pH 7.35). Ca currents were blocked by the addition of 10 µM nifedipine in the bath solution and the slow delayed rectifier K current (I_{Ks}) was blocked with 10 µM chromanol. The pipette solutions contained (in mM): 140 KCl, 10 HEPES, 11 EGTA, 1 $MgCl_2$, 1 $CaCl_2$, 5 MgATP, and 5 K_2ATP; the pH adjusted to 7.2 with KOH. Currents were recorded in the whole-cell, voltage clamp configuration of the patch-clamp technique using an Axopatch-200B amplifier (Axon Instruments, Inc., Burlingame, CA). IKr was recorded using a short 200 ms depolarizing pulse from a holding potential of -40 mV and test pulses were applied at various voltages from -40 to +40 mV in a 10 mV increment prior to returning to -40 mV for tail current recording. Measurements were repeated every two minutes to allow for complete tail current deactivation. Action potentials were recorded from single ventricular myocytes in current-clamp mode by passing depolarizing currents at subthreshold (1.4 X) intensity.

Western blots analysis: Un-transfected and transfected HEK293 cells stably expressing HERG/Kv11.1 channels were harvested and lysed in RIPA buffer (25mM Tris-HCl (pH 7.6), 150mM NaCl, 1% NP-40, 1% sodium deoxycholate, 0.1% SDS) for 30 minutes at 4°C and centrifuged at 14,000 rpm for 15 minutes. Likewise, guinea-pig ventricles were minced in RIPA buffer and homogenized with a Polytron Homogenizer. After a 30 minutes incubation at 4°C, the homogenate was centrifuged at 14,000 rpm for 15 minutes. The supernatant after centrifugation was resolved by SDS-PAGE on a 4-15% Tris-HCl gel (Bio-Rad) and transferred on PVDF membrane (Bio-Rad). Blots were blocked with 5% milk for an hour and probed with HERG/Kv11.1 antibody (Sigma; 1:200), IgG (1:100) and GAPDH antibody (Sigma; 1:5000) overnight at 4°C. It was further probed with anti-rabbit IgG HRP (Santa Cruz) and anti-Human

IgG antibody (Jackson Immunolab) at a 1:5000 and 1:10,000 dilution. The signal was detected with Clarity ECL substrate (Bio-Rad) and blots were scanned in a C-Digit blot scanner (LI-COR) at high sensitivity to obtain the image. Because HERG channel delineates Human K channel, we used Kv11.1 to indicate the ERG K channel from guinea-pigs.

Guinea-pigs immunization: Antibody levels were checked at days 14, 28 and 42 by ELISA as described below. The ECG was recorded from slightly anesthetized (2-4% isoflurane) guinea-pigs in lead II and analyzed using a digital acquisition and analysis system (Power Lab/4SP). QTc was calculated using Bazett's formula as it is more suitable for anesthetized guinea-pigs[3].

ELISA: Briefly, wells were coated overnight with 0.2 µg of 52Ro protein in PBS, washed with PBS containing 0.05% Tween 20 (PBS Tween), blocked with 3% BSA/PBS Tween, washed with PBS Tween, and incubated with serial dilutions of antibody in PBS Tween (1/100, 1/500, and 1/1000) for 1 h at 22 ^{o}C. Goat anti-guinea-pig IgG conjugated to alkaline phosphatase was used at the second stage for 1 hour at 22 ^{o}C. OD was read at 405 nm. Results were considered positive if they are >2 SD greater than the mean obtained with sera prior to immunization. The peptide (GNMEQPHMDSRIGWLHNLGDQIGKPYNSSGL) corresponding to the pore forming region of HERG channel α_1 subunit was synthesized by GenScript (Piscataway, NJ) at >90% purity. ELISA using patients' sera and the peptide was performed as above except for the use of goat anti-Human IgG.

References:

1. Rautaharju PM, Surawicz B, Gettes LS, Bailey JJ, Childers R, Deal BJ, Gorgels A, Hancock EW, Josephson M, Kligfield P, Kors JA, Macfarlane P, Mason JW, Mirvis DM, Okin P, Pahlm O, van Herpen G, Wagner GS and Wellens H. AHA/ACCF/HRS recommendations for the standardization and interpretation of the electrocardiogram: part IV: the ST segment, T and U waves, and the QT interval: a scientific statement from the American Heart Association Electrocardiography and Arrhythmias Committee, Council

on Clinical Cardiology; the American College of Cardiology Foundation; and the Heart Rhythm Society. Endorsed by the International Society for Computerized Electrocardiology. *Journal of the American College of Cardiology*. 2009;53:982-91.

2. Wang J, Salata JJ and Bennett PB. Saxitoxin is a gating modifier of HERG K+ channels. *The Journal of general physiology*. 2003;121:583-98.

3. Hamlin RL, Kijtawornrat A, Keene BW and Hamlin DM. QT and RR intervals in conscious and anesthetized guinea pigs with highly varying RR intervals and given QTc-lengthening test articles. *Toxicol Sci*. 2003;76:437-42.